

# REPORT DOCUMENTATION PAGE

Form Approved  
OMB No. 074-0188

Public reporting burden for this collection of information is estimated to average 1 hour per response, including the time for reviewing instructions, searching existing data sources, gathering and maintaining the data needed, and completing and reviewing this collection of information. Send comments regarding this burden estimate or any other aspect of this collection of information, including suggestions for reducing this burden to Washington Headquarters Services, Directorate for Information Operations and Reports, 1215 Jefferson Davis Highway, Suite 1204, Arlington, VA 22202-4302, and to the Office of Management and Budget, Paperwork Reduction Project (0704-0188), Washington, DC 20503.

<b>1. AGENCY USE ONLY (Leave blank)</b>			<b>2. REPORT DATE</b> 1999	<b>3. REPORT TYPE AND DATES COVERED</b> Proceedings, March 15-17, 1999
<b>4. TITLE AND SUBTITLE</b> Stabilization and Suppression of a Diffusion Flame Behind A Step			<b>5. FUNDING NUMBERS</b> N/A	
<b>6. AUTHOR(S)</b> Fumiaki Takahashi, W. John Schmoll, and Vincent M. Belovich				
<b>7. PERFORMING ORGANIZATION NAME(S) AND ADDRESS(ES)</b> University of Dayton Research Institute 300 College Park, Dayton, Ohio 45469			<b>8. PERFORMING ORGANIZATION REPORT NUMBER</b> N/A	
<b>9. SPONSORING / MONITORING AGENCY NAME(S) AND ADDRESS(ES)</b> SERDP 901 North Stuart St. Suite 303 Arlington, VA 22203			<b>10. SPONSORING / MONITORING AGENCY REPORT NUMBER</b> N/A	
<b>11. SUPPLEMENTARY NOTES</b> No copyright is asserted in the United States under Title 17, U.S. code. The U.S. Government has a royalty-free license to exercise all rights under the copyright claimed herein for Government purposes. All other rights are reserved by the copyright owner.				
<b>12a. DISTRIBUTION / AVAILABILITY STATEMENT</b> Approved for public release: distribution is unlimited.			<b>12b. DISTRIBUTION CODE</b> A	
<b>13. ABSTRACT (Maximum 200 Words)</b> Using a flow visualization technique, stabilization and suppression of a nonpremixed methane flame behind a backward-facing step in a wind tunnel have been studied by impulsively injecting a gaseous fire-extinguishing agent into the airflow. As the mean air velocity was increased, two distinct flame stabilization and suppression regimes were observed: rim-attached wrinkled laminar flame and wake-stabilized turbulent flame. In the former, the flame detached immediately after agent arrival, while in the latter, the flame zone in the shear layer first became unstable, followed by the extinction of the flame in the recirculation zone.				
<b>14. SUBJECT TERMS</b> SERDP, SERDP Collection, fire suppression, flame stabilization			<b>15. NUMBER OF PAGES</b> 4	
			<b>16. PRICE CODE</b> N/A	
<b>17. SECURITY CLASSIFICATION OF REPORT</b> unclass	<b>18. SECURITY CLASSIFICATION OF THIS PAGE</b> unclass	<b>19. SECURITY CLASSIFICATION OF ABSTRACT</b> unclass	<b>20. LIMITATION OF ABSTRACT</b> UL	

NSN 7540-01-280-5500

Standard Form 298 (Rev. 2-89)  
Prescribed by ANSI Std. Z39-18  
298-102

20010618 029

## STABILIZATION AND SUPPRESSION OF A DIFFUSION FLAME BEHIND A STEP

Fumiaki Takahashi and W. John Schmoll

University of Dayton Research Institute

300 College Park, Dayton, Ohio 45469

E-mail: ftakahas@engr.udayton.edu

Vincent M. Belovich

Air Force Research Laboratory

Wright-Patterson Air Force Base, Ohio 45433

### ABSTRACT

Using a flow visualization technique, stabilization and suppression of a nonpremixed methane flame behind a backward-facing step in a wind tunnel have been studied by impulsively injecting a gaseous fire-extinguishing agent into the airflow. As the mean air velocity was increased, two distinct flame stabilization and suppression regimes were observed: rim-attached wrinkled laminar flame and wake-stabilized turbulent flame. In the former, the flame detached immediately after agent arrival, while in the latter, the flame zone in the shear layer first became unstable, followed by the extinction of the flame in the recirculation zone.

### INTRODUCTION

A recirculation zone formed behind a clutter in the aircraft engine nacelle, which encases the engine compressor, combustors and turbine, can stabilize fires under over-ventilated conditions [1-4]. The fuel sources are leaking jet-fuel and hydraulic-fluid lines that can feed the fire in the form of a spray or pool. Suppression occurs when a critical concentration of agent is transported to the fire. As currently-used halon 1301 (bromotrifluoromethane) fire extinguishant is replaced with a possibly less effective agent, the amount of replacement agent required for fire suppression over a range of operating conditions must be determined. Hence, it is not known whether or not the flame extinguishing data using conventional cup burner or counterflow diffusion flame methods [2, 5, 6] can characterize the bluff-body stabilized flames.

In the previous paper [7], the critical suppression limits of step-stabilized flames were reported for two different step heights and various air velocities using halon 1301 as the baseline agent. In this paper, an attempt is made to gain a better understanding of the fundamental mechanisms of flame stabilization and suppression of step-stabilized flames using a flow visualization technique.

### EXPERIMENTAL TECHNIQUES

The apparatus (Fig. 1) consists of the fuel, air, and agent supply systems, a horizontal wind tunnel (154-mm<sup>2</sup> square cross section), and a scrubber. Methane issues upward at a mean velocity of 0.7 cm/s (heat release: ~22 W) from a porous plate placed downstream of a backward-facing step (height [ $h_s$ ]: 32 mm or 64 mm). The airflow is regulated and passes through a perforated plate to generate turbulence (typically ~6%). The mean air velocities at the test section inlet ( $U_{a0}$ ) and the step ( $U_{as}$ ) are calculated by dividing the volumetric flow rate by the cross-sectional areas of the full test section and the air passage above the step, respectively.

The agent supply system, which is similar to that of Hamins, et al. [2, 3], consists of an agent reservoir, two gaseous agent storage vessels (38 l each), and computer-controlled solenoid valves. The gaseous agent is injected impulsively into the air radially ~1 m upstream of the flame. The amount of injected agent is controlled by varying the initial pressure and the time period that the valve is open and determined from the difference between the initial and final pressures in the storage vessel using the ideal-gas equation of state. The agent injection test is repeated 20 times to determine the probability of extinction. The extinction condition is confirmed at a probability of 90% chosen arbitrarily.

The schlieren system consists of a xenon flashlamp (duration: ~1  $\mu$ s), concave mirrors (15 cm dia., f10), a vertical knife-edge, and a camera. The flashlamp is synchronized with a free-running video camera set at 60 Hz or a 35-mm camera set at a known time delay after activating the agent release valve.

### RESULTS AND DISCUSSION

Figure 2 shows a schematic of the step-stabilized nonpremixed flames. Two distinct flame stabilization regimes were observed: rim-attached and wake. At low mean air velocities at the step ( $U_{as} < \sim 3$  m/s), a

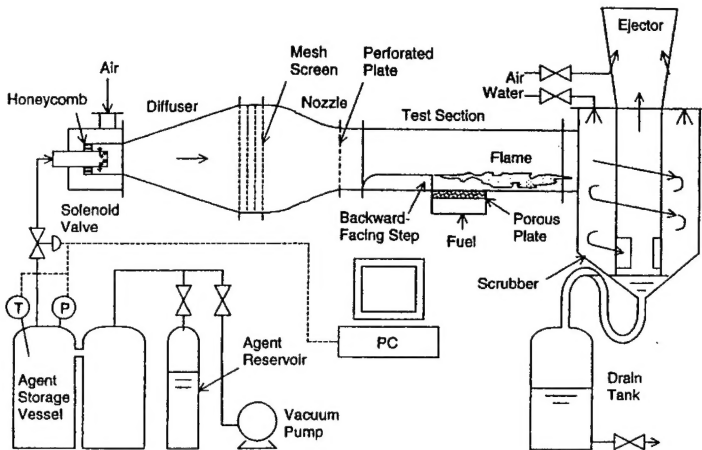


Fig. 1 Experimental apparatus.

wrinkled laminar diffusion flame attached to the edges of the backward-facing step. There existed a short ( $\sim 2$  cm) blue flame zone, with a dark space ( $\sim 1$  mm) between the flame base and the rim, and a trailing long ( $\sim 50$  cm) bright-yellow flame, typical of hydrocarbon diffusion flames. On the other hand, at high mean air velocities at the step ( $U_{a0} > \sim 8$  m/s for  $h_s = 64$  mm or immediately after detachment at 3.3 m/s for  $h_s = 32$  mm), a turbulent blue flame was stabilized  $\sim 1$  cm downstream of the rim and developed in the shear layer. Less turbulent flame zones with sporadic yellow flashes were formed in the wake of the step.

Figure 3 shows the critical agent mole fraction at suppression ( $X_c$ ) as a function of agent injection period ( $\Delta t$ ) at different mean air velocities for two different step heights [7]. As  $\Delta t$  was increased for a given  $U_{a0}$ ,  $X_c$  decreased monotonically. For a low  $U_{a0}$ , large  $X_c$  and  $\Delta t$  were required to suppress the flame. At  $U_{a0} = 0.3$  m/s, the extinction limit curves for two different step heights were nearly coincident. For higher air velocities, the minimum agent mole fraction below which no extinction occurred even at long injection periods: for  $U_{a0} = 7.1$  m/s,  $X_c = 0.025$  for both step heights. This agent concentration threshold is roughly consistent with the minimum agent concentration of  $\sim 3\%$  obtained using a cup burner and counterflow diffusion flames at a low strain rate ( $50\text{ s}^{-1}$ ) [2, 5]. Furthermore, there existed a minimum injection period, below which the flame could not be extinguished even at high agent concentrations:  $\Delta t \approx 0.05$  s for  $h_s = 32$  mm and  $\Delta t \approx 0.1$  s for  $h_s = 64$  mm.

The extinction-limit curves for step-stabilized flames at high air velocities can be explained [7] in terms of a phenomenological model for a well-stirred reactor originated by Longwell, et al. [8] and further

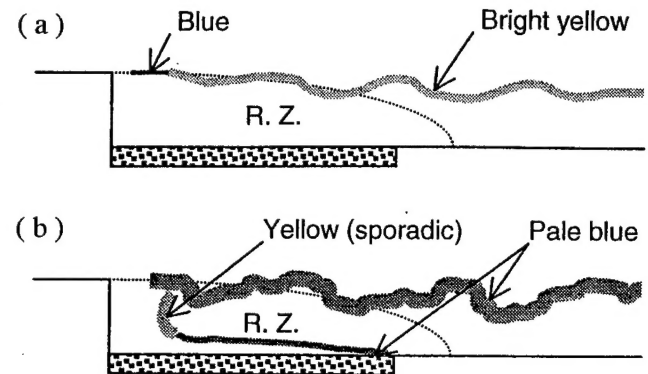


Fig. 2 Flame stabilization and suppression regimes. (a) Rim-attached flame, (b) wake-stabilized flame. R. Z.: recirculation zone.

developed by Hamins, et al [4]. It was assumed that the flame was stabilized in the recirculation zone downstream of the step. To extinguish the flame, the agent mole fraction in the recirculation zone had to reach a critical value ( $X_\infty$ ), and the agent injection period was expressed as:

$$\Delta t = -\tau \ln(1 - X_\infty)$$

The theoretical curves showed a general trend obtained experimentally; the curves for  $\tau = 0.1$  and 0.2 generally followed the data points for  $h_s = 32$  mm and 64 mm, respectively.

Figures 4 through 6 show the selected instantaneous schlieren images (from 35 mm slide films) of the flame behind the 32 mm step at the event of suppression at three different inlet air velocities ( $U_{a0} = 1.4, 2.9$ , and  $7.1$  m/s). The flame in Fig. 4 is in the rim-attached regime and those in Figs. 4 and 6 are in the wake regime. The direct (yellow) emission from the attached flame is also seen in Fig. 4a. The agent was released into the airflow for 0.25 s. At 0.49 s after agent injection ( $t_{\text{inj}} + 0.49$  s), the high-molecular-weight (149) agent has just arrived in the test section, showing fine irregularity in the upper airflow of the image. The agent appears to be fairly well dispersed into the airflow. The hot boundary on the upper side of the flame shows the large-scale vortical nature of the wrinkled flame, while the lower side shows a thick smooth boundary, typical of laminar diffusion flames. At  $t_{\text{inj}} + 0.54$  s (Fig. 4b), the flame base is moving downstream, and at  $t_{\text{inj}} + 0.63$  s (Fig. 4c), the flame is  $\sim 30$  mm detached from the step, becoming a more turbulent wake flame. The detached flame drifted away further downstream (not shown) and eventually blew off if the partially premixed flame could not propagate back to the step.

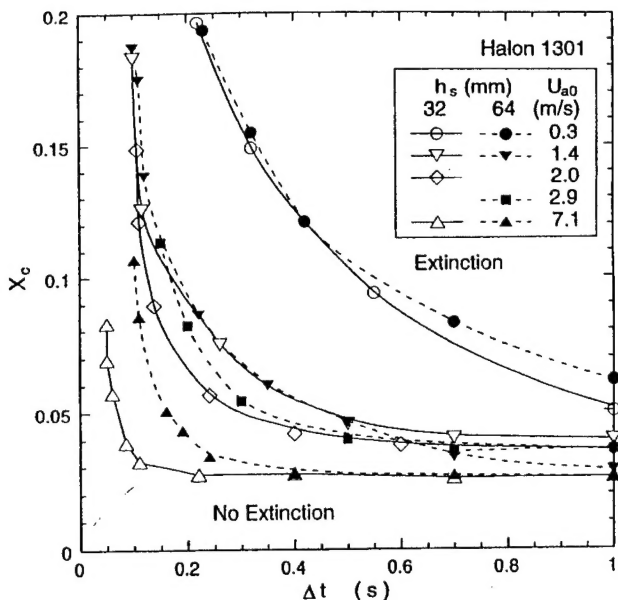


Fig. 3 The critical agent mole fraction at suppression vs. agent injection period.

At a higher inlet air velocity (Fig. 5a), the detached flame appeared to have a more violent wavy structure in the shear layer and a separate flame was formed in the recirculation zone over the porous plate (appeared as an inclined dark-bright boundary in the image). The agent arrived in the test section just at  $t_{inj} + 0.26$  s, showing the irregularity in the left half of the airflow in the image. At  $t_{inj} + 0.29$  s (Fig. 5b), the flame zone in the shear layer became unstable, while the flame in the recirculation zone was still burning. At  $t_{inj} + 0.40$  s (Fig. 5c), the wake flame was almost extinguished, showing the shear layer vortices visualized by the remaining hot gases and the agent-laden free air flow.

At the highest inlet air velocity (Fig. 6a), the small-scale turbulence coexisted with the large-scale vortices in the shear layer where the turbulent flame was formed. The less turbulent flame in the recirculation zone was also visualized. The time  $t_{inj} + 0.145$  s was just before the agent arrival, and thus the upper region was almost uniform. At  $t_{inj} + 0.150$  s (Fig. 6b), the agent arrived and the shear layer flame was already affected. At  $t_{inj} + 0.15$  s (Fig. 6b), the agent arrived and the shear layer flame was already affected. At  $t_{inj} + 0.26$  s (Fig. 6c), the flame was already extinguished and the small-scale turbulence, typical of cold shear layers, was visualized by the agent-laden airflow. The extinction timing is consistent with the aforementioned theory predicting the turbulent mixing time ( $\sim 0.1$  s) to reach the critical agent mole fraction in the recirculation zone.

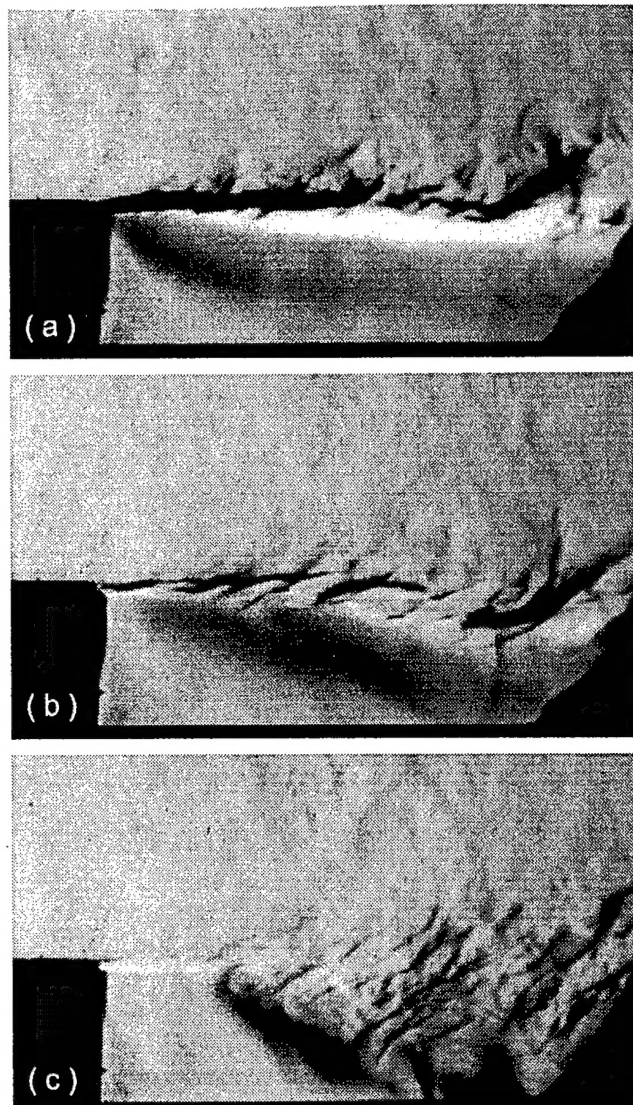


Fig. 4 Schlieren photographs.  $U_{a0} = 1.4$  m/s. (a)  $t_{inj} + 0.49$  s, (b)  $t_{inj} + 0.54$  s, (c)  $t_{inj} + 0.63$  s.

## CONCLUSIONS

The optical observations of nonpremixed methane flames stabilized by a backward-facing step in an airstream were reported using a gaseous suppressant (halon 1301). Two distinct regimes of flame stabilization and, in turn, suppression mechanisms were observed: (I) rim-attached wrinkled laminar flame and (II) wake-stabilized turbulent flame. In regime I, the flame detached from the step immediately after the agent arrival in the flame region and blew off. In regime II, the turbulent flame in the shear layer became unstable and then the flame in the recirculation zone extinguished. The extinction timing observed is consistent with the theoretical consideration of the turbulent mixing and extinction process in the recirculation zone.

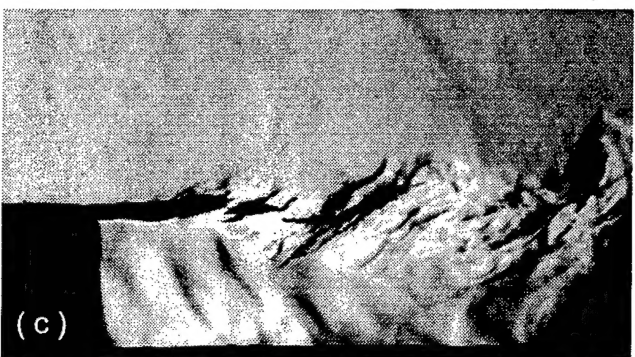
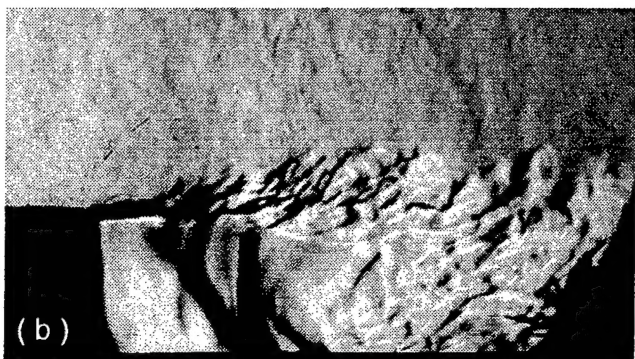


Fig. 5 Schlieren photographs.  $U_{a0} = 2.9$  m/s. (a)  $t_{inj} + 0.26$  s, (b)  $t_{inj} + 0.29$  s, (c)  $t_{inj} + 0.40$  s.

#### ACKNOWLEDGMENT

This research is part of the Department of Defense's Next-Generation Fire Suppression Technology Program, funded by the DoD Strategic Environmental Research and Development Program and the Air Force Research Laboratory, Propulsion Directorate, Propulsion Sciences and Advanced Concept Division, Wright-Patterson Air Force Base, Ohio, under Contract No. F33615-97-C-2719 (Technical Monitor: C. W. Frayne).

#### REFERENCES

1. Grosshandler, W. L., Gann, R. G., and Pitts, W. M., *NIST SP 861*, 1994, pp. 1-12.
2. Hamins, A., Gmurczyk, G., Grosshandler, W., Rehwoldt, R. G., Vazquez, I., Cleary, T., Presser,

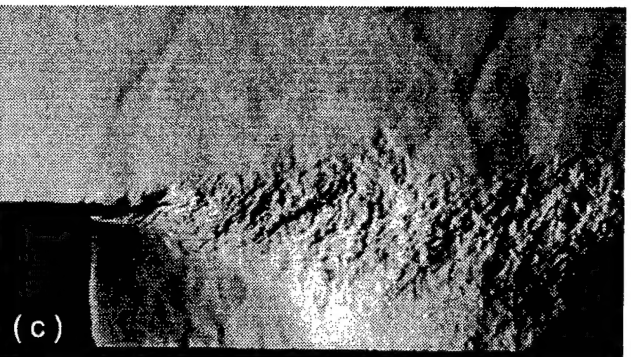
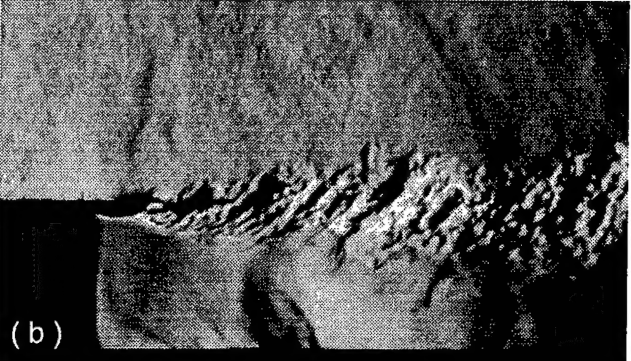
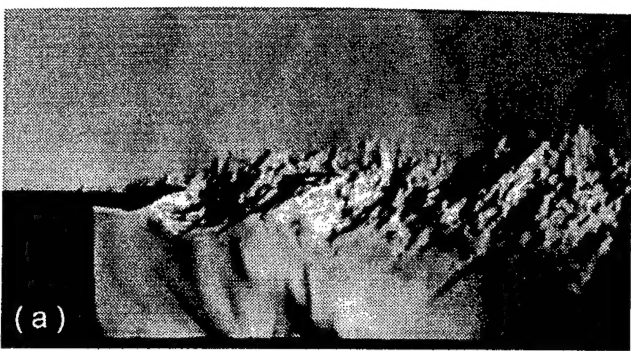


Fig. 6 Schlieren photographs.  $U_{a0} = 7.1$  m/s. (a)  $t_{inj} + 0.145$  s, (b)  $t_{inj} + 0.15$  s, (c)  $t_{inj} + 0.26$  s.

C., and Seshadri, K., *ibid.*, 1994, pp. 345-465.

3. Hamins, A., Cleary, T., Borthwick, P., Gorchkov, N., McGrattan, K., Forney, G., Grosshandler, W., Presser, C., and Melton, L., *NIST SP 890: Vol. II*, 1995, pp.1-199.
4. Hamins, A., Presser, C., and Melton, L., *26th Symp. (Int'l) on Combust.*, 1996, pp. 1413-1420.
5. Hamins, A., Trees, D., Seshadri, K., and Chelliah, H. K., *Combust. Flame* 99: 221-230 (1994).
6. Saso, Y., Saito, N., Liao, C., and Ogawa, Y., *Fire Safety Journal* 26: 303-326 (1996).
7. Takahashi, F., Schmoll, W. J., and Belovich, V. M., *AIAA Paper No. 98-3529*, 1998.
8. Longwell, J. P., Frost, E. E., and Weiss, M. A., *Indust. Eng. Chem.* 45: 1629-1637 (1953).